

Electronic structures of graphane with vacancies and graphene adsorbed with fluorine atoms

Bi-Ru Wu and Chih-Kai Yang

Citation: *AIP Advances* **2**, 012173 (2012); doi: 10.1063/1.3696883

View online: <http://dx.doi.org/10.1063/1.3696883>

View Table of Contents: <http://aipadvances.aip.org/resource/1/AAIDBI/v2/i1>

Published by the [American Institute of Physics](http://www.aip.org).

Related Articles

Strong current polarization and negative differential resistance in chiral graphene nanoribbons with reconstructed (2,1)-edges

Appl. Phys. Lett. **101**, 073101 (2012)

Ab initio study of the interactions between boron and nitrogen dopants in graphene

J. Appl. Phys. **112**, 034304 (2012)

Band gaps and structural properties of graphene halides and their derivatives: A hybrid functional study with localized orbital basis sets

J. Chem. Phys. **137**, 034709 (2012)

Abnormal pseudospin-degenerate states in a graphene quantum dot with double vacancy defects

J. Appl. Phys. **112**, 014308 (2012)

Electronic band gaps and transport in aperiodic graphene superlattices of Thue-Morse sequence

Appl. Phys. Lett. **100**, 252402 (2012)

Additional information on AIP Advances

Journal Homepage: <http://aipadvances.aip.org>

Journal Information: <http://aipadvances.aip.org/about/journal>

Top downloads: http://aipadvances.aip.org/most_downloaded

Information for Authors: <http://aipadvances.aip.org/authors>

ADVERTISEMENT



AIPAdvances

Now Indexed in Thomson Reuters Databases

Explore AIP's open access journal:

- Rapid publication
- Article-level metrics
- Post-publication rating and commenting

Electronic structures of graphane with vacancies and graphene adsorbed with fluorine atoms

Bi-Ru Wu¹ and Chih-Kai Yang^{2,a}

¹Center for General Education, Chang Gung University, Kueishan, Taiwan

²Graduate Institute of Applied Physics, National Chengchi University, Taipei 11605, Taiwan

(Received 16 November 2011; accepted 22 February 2012; published online 13 March 2012)

We investigate the electronic structure of graphane with hydrogen vacancies, which are supposed to occur in the process of hydrogenation of graphene. A variety of configurations is considered and defect states are derived by density functional calculation. We find that a continuous chain-like distribution of hydrogen vacancies will result in conduction of linear dispersion, much like the transport on a superhighway cutting through the jungle of hydrogen. The same conduction also occurs for chain-like vacancies in an otherwise fully fluorine-adsorbed graphene. These results should be very useful in the design of graphene-based electronic circuits. *Copyright 2012 Author(s). This article is distributed under a Creative Commons Attribution 3.0 Unported License.* [<http://dx.doi.org/10.1063/1.3696883>]

Graphane^{1,2} is a single sheet of graphene fully adsorbed with hydrogen atoms, with each carbon atom bonded to an H atom alternately on either side of the layer. Graphane is known to have a large band gap³ around 3.5 eV and is more chemically inert compared with the pristine graphene. However, it is always possible that a small amount of H vacancies remains after a hydrogenation process or occurs by means of physical or chemical desorption. Magnetism caused by vacancies in graphane attracts much interest.⁴⁻⁷ In addition, such a distribution of vacancies has the potential to alter the conduction property drastically and find application in the growing field of graphene-based nanoelectronics.⁷⁻¹¹

Fluorine atoms are also known to bond to graphene strongly. A graphene layer fully adsorbed with F atoms¹² is also a semiconductor with a large band gap, making the composite chemically stable but difficult for application in nanoelectronic circuits. It is thus a natural extension to explore what roles F vacancies may play in F-adsorbed graphene.^{13,14} In this paper we report our systematic investigation of various distributions of vacancies on both H and F-adsorbed graphene and how they affect the overall physical properties.

We use density functional calculation as the main tool for the research. The calculation is based on the projector augmented wave potentials implemented in the *ab initio* VASP code¹⁵⁻¹⁸ with generalized gradient approximation. For exchange-correlation functional, the version of Perdew, Burke and Ernzerhof¹⁹ is adopted. Energy cutoff is set at 500 eV. A $9 \times 9 \times 1$ Monkhorst-Pack k-point mesh is used for the sampling of k points in the Brillouin zone. By allowing relaxation of the size of the unit cell as well as relative positions of atoms, we derive an optimal lattice constant of 2.545 Å for pure graphane and 2.578 Å for graphane fully adsorbed with F atoms. To accommodate vacancies a unit cell consisting of 32 C atoms and 32 adsorbed impurities is adopted. For bigger vacancy clusters, an even larger unit cell with 50 atoms for each species is used. Adjacent to the atomic layer is added a vacuum slab with thickness of 15 Å, which, after repeated tests with much larger lengths, proves sufficient for the relaxation of adsorbed atoms and avoids the interaction between neighboring atomic layers. All configurations are subject to relaxation until the force acting on each atom is less than 0.05 eV/Å.

^aElectronic mail: ckyang@nccu.edu.tw



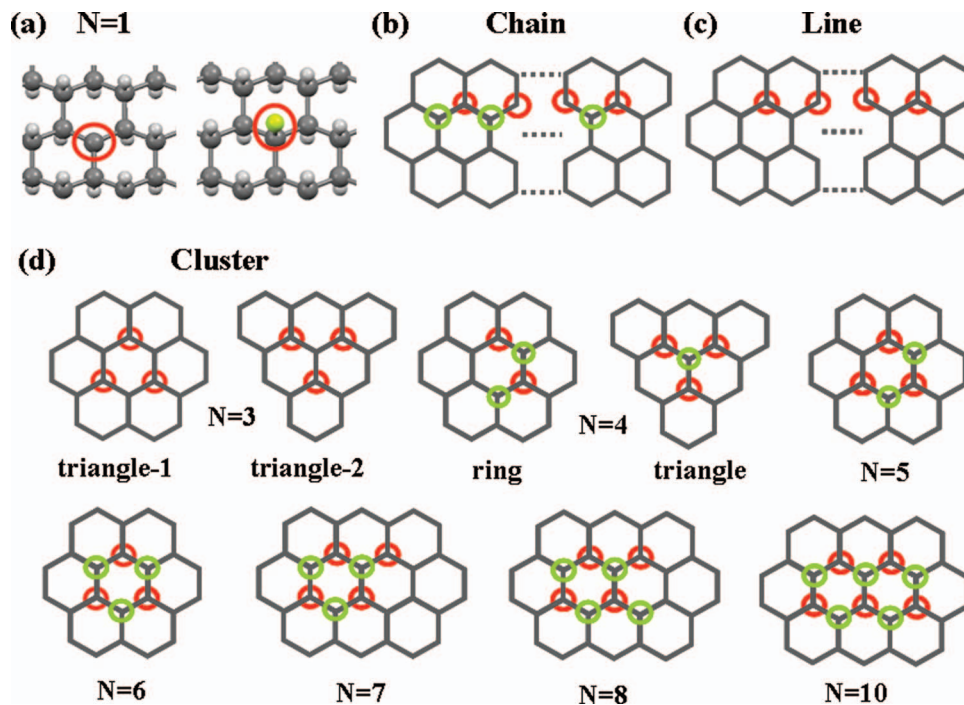


FIG. 1. Configurations of chains, lines, and clusters considered in the calculation. Circles represent positions of vacancies or adsorbed F atoms. Red (dark) and green (gray) circles denote F atoms adsorbed on different sides. Single vacancy and adsorbed F are shown in the left and right side of (a) respectively.

Fig. 1 gives a depiction of many of the configurations included in our calculation. A single H vacancy and an adsorbed F atom filling the place are considered (Fig. 1(a)). For vacancy numbers larger than two we use chains, lines and clusters to describe the configurations. A zigzag distribution of H vacancies is called a vacancy chain and their filling by F atoms called F chain (Fig. 1(b)). The latter has F atoms connected to C atoms alternately on either side of graphene. Linear distribution of H vacancies or adsorbed F atoms filling the same H vacancies is called a line (Fig. 1(c)). An F line has all its F atoms present on one side of the graphene. Finally, clusters are all compact aggregations of H vacancies or adsorbed F except in the case of three vacancies (F atoms) (Fig. 1(d)). Neighboring F atoms in a cluster appear alternately on either side of the carbon layer. There are two cluster types in the case of four vacancies or adsorbed F, a ring and a triangle.

Formation energies for lines, chains, and clusters of H vacancies are plotted in Fig. 2(a). Formation energy of an H vacancy is calculated by $E_f = [E_{\text{tot}}(\text{graphane with } N_{\text{vac}} \text{ H vacancies}) - E_{\text{tot}}(\text{pure graphane}) + N_{\text{vac}} \times E_{\text{tot}}(\text{one free H atom})] / N_{\text{vac}}$, where N_{vac} is the number of H vacancies and E_{tot} is the total energy of the configuration enclosed in the parenthesis. As is clearly shown in the figure, it is much easier to form H vacancies in clusters or chains than in lines. The difference is usually more than 1 eV per vacancy. There is also a slight advantage for forming a cluster in closed ring (such as $N = 6$) than a chain. We expand the unit cell to accommodate a larger cluster or chain in some cases and the trend remains. Since the distance between two nearest vacancies in a line is much larger than that between two nearest vacancies in a chain or cluster, it clearly indicates that a patch of neighboring vacancies is favored over disconnected ones. Formation energy for the ring type of $N = 4$ is lower than the triangle type by 0.35 eV/vacancy.

For F atoms taking H vacancies the trend is completely reversed. Shown in Fig. 2(b) is a plot of adsorption energy per F atom against the number of adsorbed F atoms. Adsorption energy of an F atom taking place of an H vacancy is $E_{\text{ad}} = [E_{\text{tot}}(\text{graphane adsorbed with } N_F \text{ F atoms}) - E_{\text{tot}}(\text{graphane with } N_{\text{vac}} \text{ H vacancies}) - N_F \times E_{\text{tot}}(\text{one free F atom})] / N_F$, where N_F is the number of adsorbed F atoms. F atoms in clusters and chains, which are crammed into tighter space and hence more repulsive to each other, tend to be more difficult to be adsorbed than those in a line. For example, adsorption

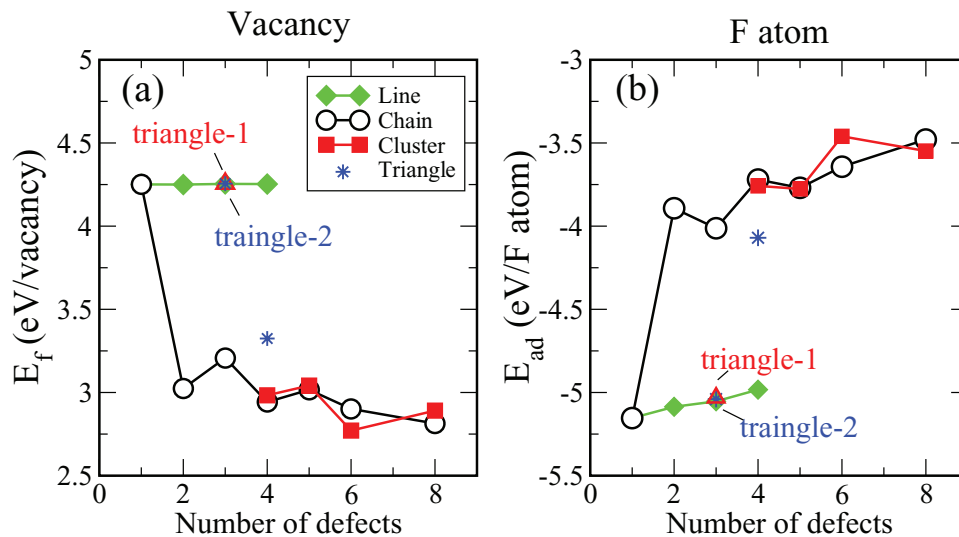


FIG. 2. (a) Formation energies for chains, lines, and clusters of H vacancies in graphane. (b) Adsorption energy per F atom taking the same H vacancies.

energy for the ring type of $N=4$ is higher than that of the triangle type. The more so the more adsorbed F atoms. But the relatively large absolute values of adsorption energies in all cases confirm strong bonding between C and F atoms.

Next we turn to the electronic structure of the calculation. An isolated H vacancy represents an unpaired electron in the dangling bond extending from the C, thus producing a magnetic moment of $1 \mu_B$.²⁰ This is the common starting point of all subsequent calculations on configurations related to H vacancies. For odd numbers of nearest-neighbor vacancies, such as those in chains and clusters, there is always one unpaired electron and a total magnetic moment of $1 \mu_B$ per unit cell. For unit cells containing even number of nearest-neighbor vacancies, complete pairing of electrons produces no net moment except in lines of vacancies. However, the triangle type consisting of four H vacancies shows different behavior. Because three of the H vacancies are not adjacent to one another, only one pairing of electrons is possible and a total magnetic moment of $2 \mu_B$ is produced in the unit cell. As to the line configuration shown in Fig. 1, H vacancies in lines are not adjacent to each other and therefore contribute parallel magnetic moments proportional to the number of vacancies in the unit cell. For the same reason, the unit cell containing 3 triangular vacancies also possesses a moment of $3 \mu_B$.

As typical examples we illustrate in Fig. 3 and 4 band structure, density of states (DOS) and local density of states (LDOS) of vacancies for an odd ($N=3$) and even number ($N=4$) of vacancies respectively. Spin polarized impurity states can be identified in all three configurations in Fig. 3(a). For the chain configuration two almost dispersionless defect states are found within 1 eV below and above the Fermi level, corresponding to the majority and minority spin respectively. For the other two configurations, spin-polarized defect states are also found on either side of the Fermi level. But only in the three vacancies in line can one find slight dispersion in the defect states. Although there is a distinct possibility of optical transition between defect states on either side of the Fermi level, there is virtually no electric transport possible for graphane with isolated H vacancies. Fig. 3(b) provides spin-polarized DOS and LDOS for defects of the three configurations. In Fig. 4(a) defect states are spin-polarized for the triangle and line configurations. The chain and cluster display no magnetism and produce more separated defect states. DOS and LDOS of the four configurations are depicted in Fig. 4(b).

When H vacancies are occupied by fluorine atoms, as are shown in the configurations related to F in Fig. 1, impurity states caused by F atoms are generally deep below or well above the Fermi level and thus play no part in the transport property. A typical example of F adsorption is provided

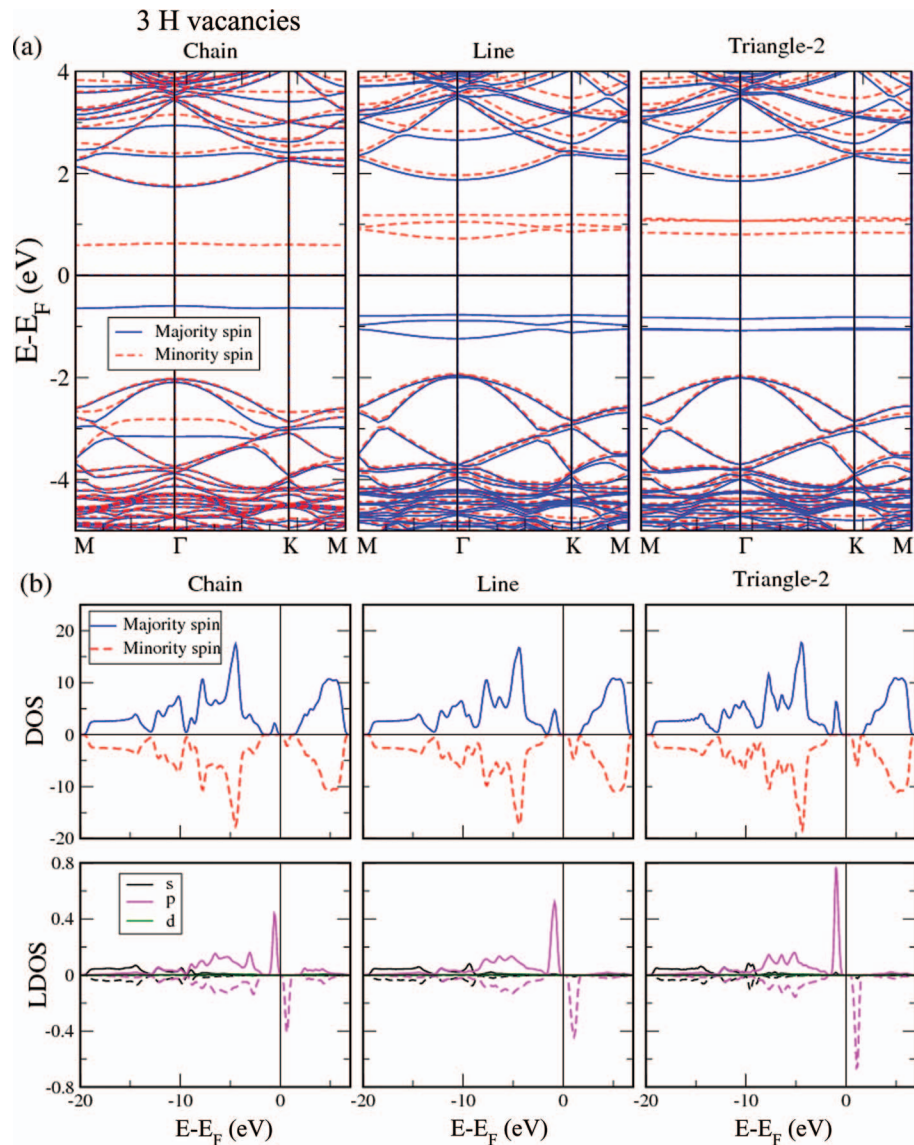


FIG. 3. (a) Band structure for configurations with a chain, line, and triangle of three H vacancies. (b) DOS and LDOS for the same H vacancies.

by Fig. 5, where impurity states of the three F atoms in a chain, line, and triangle are shown. Most are well below -2 eV and graphene valence bands or close to 4 eV above the Fermi level. There is even an increase of band gap as a result of the adsorption of F atoms. This is in agreement with the large adsorption energy and chemical inertness associated with F.

One surprise comes from the configuration of a continuous chain of H vacancies. For the continuous chain we also try a rectangular supercell and allow it to relax in size in the lateral direction. The results are similar to the unrelaxed supercell, including the electronic structure in the low energy region and magnetic property. Found in the band structure (Fig. 6(a)) are crossing bands centered on Γ point, with linear valence and conduction bands converged at the Fermi level. The crossing bands are mainly populated by the p orbitals (88 % at Γ point) of the continuous carbon chain not bonded to H. This is in sharp contrast to pure graphene, whose Dirac points are at K and K' . Thus graphene with a continuous chain of H vacancies is a conductor providing linear transport

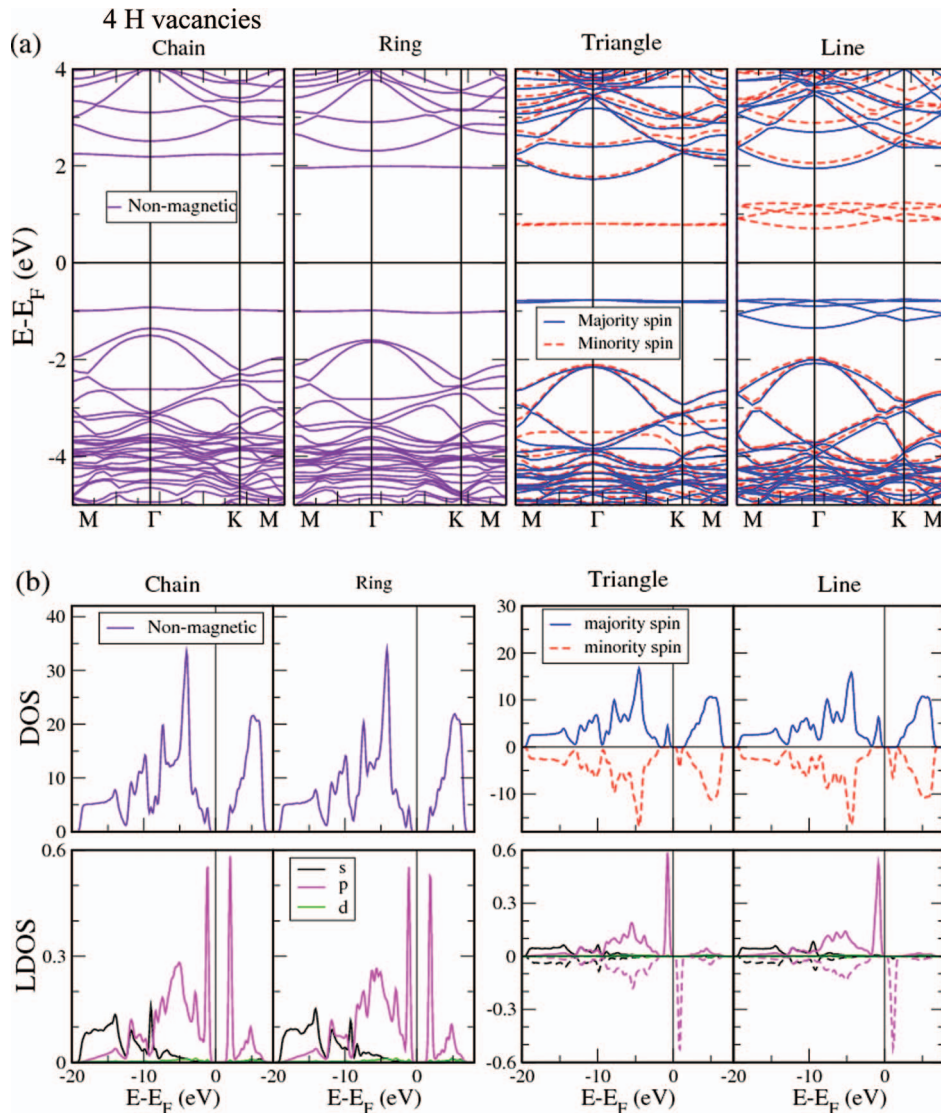


FIG. 4. (a) Band structure for configurations with four H vacancies. (b) DOS and LDOS for the same H vacancies.

through the jungle of H atoms. However, if the vacancies are filled with F atoms, the whole structure relapses into a high band-gap (4.230 eV) semiconductor.

Similar linear dispersion also occurs for a chain of vacancies in a graphene layer that is otherwise adsorbed with F atoms, as is shown in Fig. 6(b). Interestingly, if the chain of vacancies is in graphene adsorbed with H on one side and F on the other, a small energy gap of 0.106 eV is generated, separating the valence bands from the conduction bands (Fig. 6(c)). Apparently the gap is caused by symmetry breaking as a result of the heterogeneous adsorption.

Finally we consider configurations in which two continuous chains of vacancies come across each other, as is shown in Fig. 7. Calculation shows that a gap developed as a result of defect bands repelling each other. For crossing chains in graphene the gap (0.231 eV) is the smallest compared with that of graphene with one side adsorbed with H and another with F (0.442 eV) or graphene with both sides adsorbed with F (0.379 eV).

In conclusion, H vacancies in graphene produce defect states that appear in the graphene band gap. Magnetic moments can also be generated depending on whether there are unpaired electrons in the configuration. H vacancies filled with F atoms, however, generate deep impurity states. A

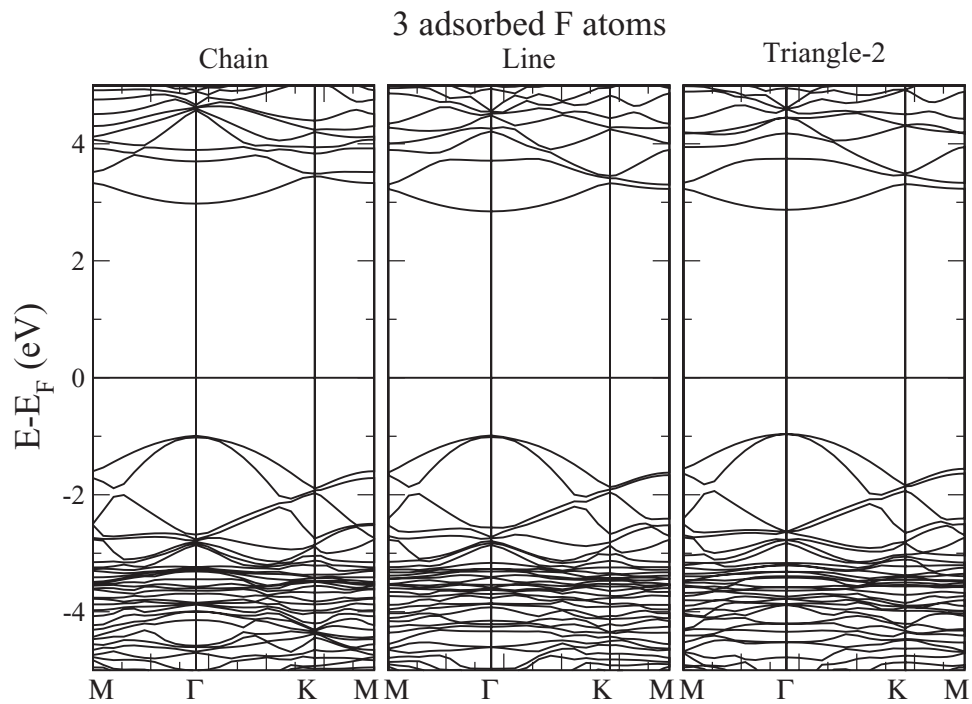


FIG. 5. Impurity states for three F atoms filling the H vacancies.

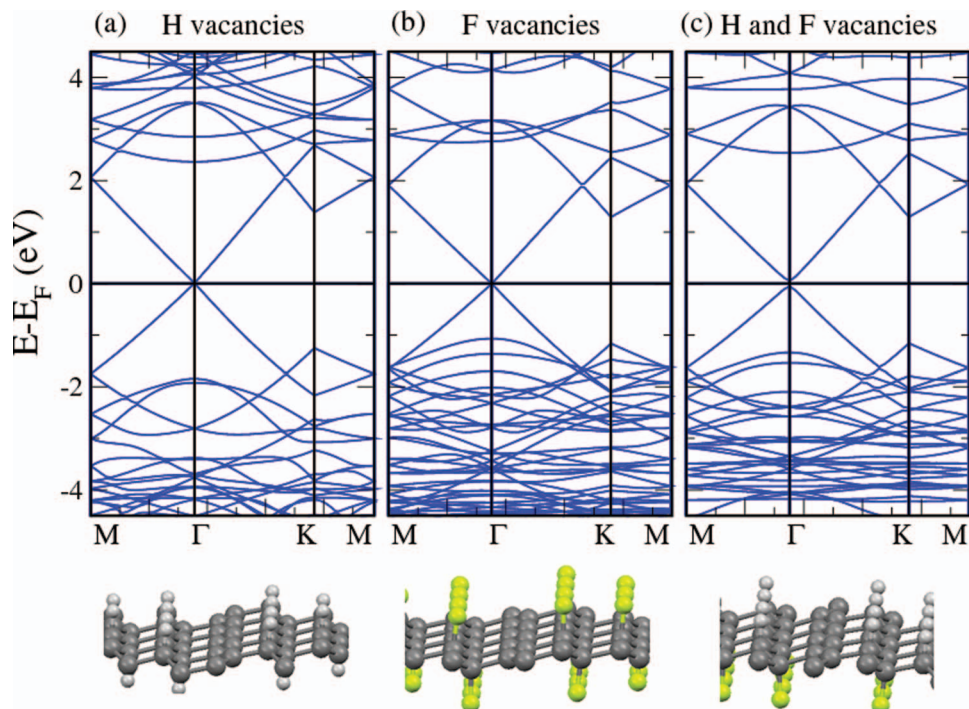


FIG. 6. Linear crossing bands are formed at Γ point for a continuous chain of H vacancies in a graphene layer otherwise adsorbed with H (a) or F (b) atoms. If the layer is adsorbed with H on one side and F on the other, the chain of vacancy will result in a small gap (c).

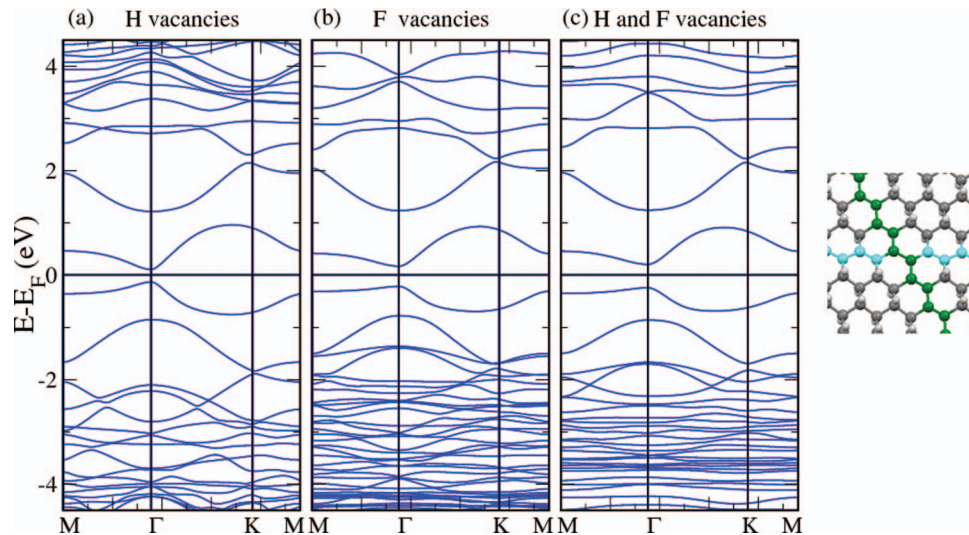


FIG. 7. Band structure for two continuous chains of vacancies crossing each other in a layer adsorbed with H (a), F (b) atoms, and (c) H on one side and F on the other.

continuous chain of vacancies in H or F adsorbed graphene turns the structure into a conductor of linear dispersion. These results should be useful in designing nanoelectronic circuits based on graphene.

ACKNOWLEDGMENTS

This work was supported by the National Science Council of the Republic of China under contract number NSC 98-2112-M-004-003-MY3. Supports from the National Centers for Theoretical Sciences and High-performance Computing of the ROC are also gratefully acknowledged.

- ¹D. C. Elias, R. R. Nair, T. M. G. Mohiuddin, S. V. Morozov, P. Blake, M. P. Halsall, A. C. Ferrari, D. W. Boukhvalov, M. I. Katsnelson, A. K. Geim, and K. S. Novoselov, *Science* **323**, 610 (2009).
- ²A. Savchenko, *Science* **323**, 589 (2009).
- ³J. O. Sofo, A. S. Chaudhari, and G. D. Barber, *Phys. Rev. B* **75**, 153401 (2007).
- ⁴H. Şahin, C. Ataca, and S. Ciraci, *Appl. Phys. Lett.* **95**, 222510 (2009).
- ⁵J. Berashevich and T. Chakraborty, *Nanotechnology* **21**, 355201 (2010).
- ⁶J. Zhou, Q. Wang, Q. Sun, X. S. Chen, Y. Kawazoe, and P. Jena, *Nano Lett.* **9**, 3867 (2009).
- ⁷J. Berashevich and T. Chakraborty, *Phys. Rev. B* **82**, 134415 (2010).
- ⁸A. K. Singh, E. S. Penev, and B. I. Yakobson, *ACS Nano* **4**, 3510 (2010).
- ⁹Y. Wang, X. Xu, J. Lu, M. Lin, Q. Bao, B. Özyilmaz, and K. P. Loh, *ACS Nano* **4**, 6146 (2010).
- ¹⁰D. Haberer, D. V. Vyalikh, S. Taioli, B. Dora, M. Farjam, J. Fink, D. Marchenko, T. Pichler, K. Ziegler, S. Simonucci, M. S. Dresselhaus, M. Knupfer, B. Büchner, and A. Grüneis, *Nano Lett.* **10**, 3360 (2010).
- ¹¹R. Balog, B. Jørgensen, L. Nilsson, M. Andersen, E. Rienks, M. Bianchi, M. Fanetti, E. Lægsgaard, A. Baraldi, S. Lizzit, Z. Sljivancanin, F. Besenbacher, B. Hammer, T. G. Pedersen, P. Hofmann, and L. Hornekær, *Nat. Matter.* **9**, 315 (2010).
- ¹²P. V. C. Medeiros, A. J. S. Mascarenhas, F. de Brito Mota, and C. M. C. de Castilho, *Nanotechnology* **21**, 485701 (2010).
- ¹³J. T. Robinson, J. S. Burgess, C. E. Junkermeier, S. C. Badescu, T. L. Reinecke, F. K. Perkins, M. K. Zalalutdniov, J. W. Baldwin, J. C. Culbertson, P. E. Sheehan, and E. S. Snow, *Nano Lett.* **10**, 3001 (2010).
- ¹⁴J. O. Sofo, A. M. Suarez, G. Usaj, P. S. Cornaglia, A. D. Hernández-Nieves, and C. A. Balseiro, *Phys. Rev. B* **83**, 081411 (2011).
- ¹⁵G. Kresse and J. Hafner, *Phys. Rev. B* **47**, 558 (1993).
- ¹⁶G. Kresse and J. Hafner, *Phys. Rev. B* **49**, 14251 (1994).
- ¹⁷G. Kresse and J. Furthmüller, *Phys. Rev. B* **54**, 11169 (1996).
- ¹⁸G. Kresse and J. Furthmüller, *Comput. Mater. Sci.* **6**, 15 (1996).
- ¹⁹J. P. Perdew, K. Burke, and M. Ernzerhof, *Phys. Rev. Lett.* **77**, 3865 (1996).
- ²⁰Chih-Kai Yang, *Carbon* **48**, 3901 (2010).